

## Design and Fabrication of Hydrogen Sulfide (H<sub>2</sub>S) Gas Sensor Using PtSi/Porous n-Si Schottky Diode

Hossein Dehnavi Fard, Saeid Khatami\*, Nosrat Izadi<sup>1</sup>,  
Javad Koohsorkhi<sup>2</sup> and Alimorad Rashidi<sup>1</sup>

Department of Electrical Engineering, Amirkabir University of Technology,  
Hafez Street, Tehran 1591634311, Iran

<sup>1</sup>Research Institute Petroleum Industrial (RIPI), Olympic Village, Tehran 1485733111, Iran

<sup>2</sup>Department of Mechatronics Engineering, Faculty of New Sciences and Technologies,  
University of Tehran, North Kargar Street, Tehran 143951561, Iran

(Received January 13, 2012; accepted June 8, 2012)

**Key words:** hydrogen sulfide, porous silicon, gas sensor, Schottky diode, breakdown voltage, electric field, single-electron effect, Coulomb blockade effect

In this work, a gas sensor for the detection of H<sub>2</sub>S gas based on a PtSi/porous n-Si Schottky diode was fabricated. N-type Si substrates were made porous and Pt was deposited into the pores electrochemically. Pt was annealed and the resulting PtSi/porous n-Si Schottky junction exhibits a breakdown-type behavior in the reverse bias mode. The shifts in their breakdown voltage in the presence of the hydrogen sulfide (H<sub>2</sub>S) gas are mapped to the concentration of this gas in the environment. SEM images were taken to analyze the pores' structures. This sensor is able to respond to H<sub>2</sub>S gas concentrations down to 10 ppm at room temperature and atmospheric pressure and down to 1 ppm at higher temperatures (50 and 80°C). The response time of this sensor is in the range of 3 to 10 s. The recovery time of the sensor is between 20 to 45 s. The response time and recovery time depend on the H<sub>2</sub>S concentration and temperature. Responses of the sensor were tested for different polar (CO) and nonpolar (CH<sub>4</sub>) gases for comparison purposes. Only one gas plus nitrogen were allowed to enter the furnace each time and their *I-V* characteristics were determined. The sensor responds differently to these gases. However, the main objective of designing this sensor was to sense the H<sub>2</sub>S gas with different concentrations in an environment such as in the petroleum industry where this gas is predominantly present and is used to produce products such as sulfur and sulfuric acid. If there is more than one type of gas in an environment at the same time, the sensor does not determine how much concentration of what gas is present. That is the subject of a future work. The single-electron or Coulomb blockade effect seems to be the most reasonable explanation of the room-temperature sensing capability of this sensor.

---

\*Corresponding author: e-mail: khatami@aut.ac.ir

## 1. Introduction

Hydrogen sulfide ( $H_2S$ ) is a colorless, flammable, and very poisonous gas with the odor of rotten eggs at concentrations up to 100 parts per million (ppm).  $H_2S$  is most commonly obtained by its separation from sour gas, which is natural gas with a high content of  $H_2S$ . Hydrogen sulfide is a byproduct of the petroleum industry and is used to produce sulfur and sulfuric acid. The minimum  $H_2S$  concentration that a normal human being can smell is 8.2 ppm. However, an exposure to 5 ppm of  $H_2S$  for about 5 h can cause death. Moreover, a prolonged exposure to  $H_2S$  with concentrations higher than 8.2 ppm can numb the sense of smell and cause death.<sup>(1,2)</sup> Thus far, a variety of  $H_2S$  sensors have been fabricated, which mostly operate at elevated temperatures.<sup>(3,4)</sup> This work introduces the fabrication of an  $H_2S$  sensor, which uses a PtSi/porous n-Si Schottky diode operating in the breakdown region at room and higher temperatures. The breakdown-type behavior of PtSi/porous n-Si Schottky diodes has been attributed to the single-electron or Coulomb blockade effect and subsequent avalanche multiplication mechanisms. The single-electron or Coulomb blockade effect provides a better understanding of small-scale physics and electronics. In short, the single-electron effect is based on the fact that according to the equation  $Q = CV$ , an appreciable amount of energy (which must be larger than the thermal energy of electrons) is required to transfer a single electron into a nanostructure with a very small capacitance. For instance, it takes a threshold voltage of  $V_{th} = q/C = 1.6$  V to transfer an electron into a nanostructure with the capacitance of  $10^{-19}$  F.<sup>(5)</sup>

Both single-electron and avalanche breakdown mechanisms are caused by large fringing electric fields that are developed at tips and sharp edges of the pores, which can be orders of magnitude larger than that of a smooth area for Schottky junction under the same conditions.<sup>(6)</sup> This could result in the occurrence of breakdown at relatively low voltages, which have been seen with the PtSi/porous n-Si diodes.<sup>(6)</sup>

The PtSi/porous n-Si diode sensor employs the polar characteristics of the gases. When a gas that has an internal dipole moment fills the pores, its dipoles line up in the direction of the electric field and change the electric field distribution and magnitude, and subsequently, change the breakdown voltage of the PtSi Schottky diode sensor.<sup>(7)</sup>

## 2. Experimental

$\langle 100 \rangle$ -oriented n-type Si wafers with resistivity  $\rho$  of about 8  $\Omega$ -cm were used in this research. The Si sample size used in this research was 20 mm<sup>2</sup>. First, the samples were cleaned using the standard RCA solution. Next, the etching apparatus was placed in an ultrasonic bath and an anodic etching was performed under ultraviolet radiation in a solution containing 25 wt% HF (60%) + 15 wt% DI water + 60 wt% ethanol (99%) at  $T = 40^\circ\text{C}$ . Application of a current with the current density of 46 mA/cm<sup>2</sup> for 45 min resulted in the porous Si samples.

Percent porosity of porous samples is determined from eq. (1) and is defined as the fraction of the voids inside the porous layer vs the starting silicon. It involves the measurement of the starting weight of the sample and its weight after etching.<sup>(8)</sup>

$$P (\%) = \frac{M_1 - M_2}{M_1 - M_3} \quad (1)$$

$M_1$ ,  $M_2$ , and  $M_3$  are the weights of the wafer before the electrochemical etch, after the electrochemical etch, and after the porous layer has been removed, respectively. The removal is made through dipping the sample in an aqueous solution of KOH (3% in volume), which yields a selective removal of the porous n-Si layer without reacting with the bulk crystalline silicon.

Pt was electroplated onto the pores using a solution containing  $\text{H}_2(\text{PtCl}_6)/6\text{H}_2\text{O}$  4 g/l,  $(\text{NH}_4)_2\text{HPO}_4$  20 g/l, and  $\text{Na}_2\text{HPO}_4$  100 g/l, at  $90^\circ\text{C}$  with the application of 20 mA of current for 45 min. The samples were subsequently annealed in  $\text{N}_2$  at  $250^\circ\text{C}$  for 20 min and then at  $550^\circ\text{C}$  for 40 min to form PtSi silicide. PtSi is not known to react with the  $\text{H}_2\text{S}$  gas, particularly at the temperatures used for these sensors in this investigation. The excess unreacted Pt was removed using a HCL +  $\text{HNO}_3$  solution.<sup>(6,7,9,10)</sup>

A U-shaped quartz furnace was designed and built for this investigation for the  $\text{H}_2\text{S}$  gas sensing. The schematic picture of the test furnace is shown in Fig. 1. The gas feed consisting of  $\text{H}_2\text{S}$  gas was diluted in high-purity nitrogen (99.999%) to yield various concentrations of  $\text{H}_2\text{S}$  in the furnace. A glass bed was utilized to enhance the mixing. Nitrogen flow was controlled using a Brooks's mass flow controller (MFC) with the flow rate up to 1000 sccm. The  $\text{H}_2\text{S}$  flow was controlled using a Brooks MFC with the flow rate up to 50 sccm. Two  $\text{H}_2\text{S}$  gas cylinders with concentrations of 1000 and 200 ppm were used. The former was used to provide the furnace with  $\text{H}_2\text{S}$  concentrations of 1000 and 500 ppm after it was diluted in  $\text{N}_2$  and the latter to provide smaller concentrations of  $\text{H}_2\text{S}$  when diluted in  $\text{N}_2$ . For  $\text{H}_2\text{S}$  concentrations of 10 ppm and higher, a gas feed with a total flow rate of 100 sccm was used. For smaller concentrations of  $\text{H}_2\text{S}$  such as 1 ppm, a larger flow rate of 1000 sccm was used. This was because, to provide the furnace with 1 ppm of  $\text{H}_2\text{S}$  at the total flow rate of 100 sccm, we needed to feed 0.5% of  $\text{H}_2\text{S}$  (using

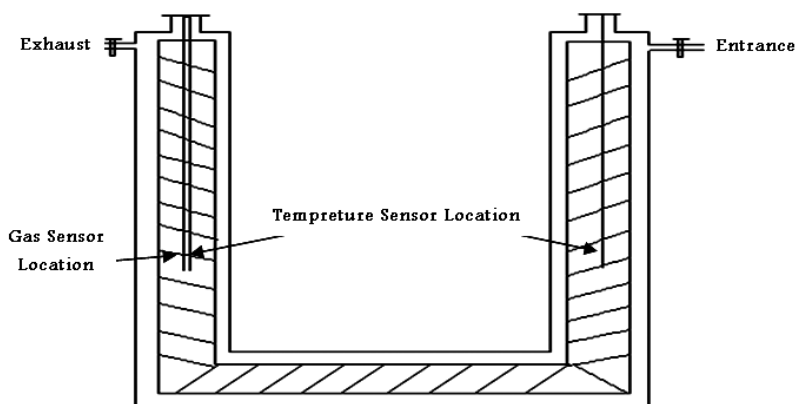


Fig. 1. Schematic of the reactor designed in this investigation for gas sensing.

a 200 ppm concentration cylinder) with 99.5% of  $N_2$  to the furnace. Reliably obtaining such a small concentration of  $H_2S$  was beyond the capability of the MFCs. To observe the effect of the temperature on the performance of the sensor, higher temperatures such as 50 and 80°C were examined in addition to room temperature. These are within the typical range of temperatures of the work environments that deal with the  $H_2S$  gas. The temperature along the entire furnace was kept constant. The reactor was kept at atmospheric pressure.  $I$ - $V$  characteristics of the diodes were obtained using Keithley data acquisition equipment. The responses of the sensor to another polar gas (CO) and a nonpolar gas ( $CH_4$ ) were also examined for comparison purposes. Only one gas plus nitrogen were allowed to enter the furnace each time and their  $I$ - $V$  characteristics were determined.

### 3. Results

Figures 2(a) and 2(b) show SEM images of a porous n-Si sample prepared for this investigation. The pore diameters were 12–18  $\mu m$  and their heights were 15–25  $\mu m$ . The pores are sharp and their distribution is relatively uniform and reproducible across the samples. The porosity level is about 75%.

Figures 3(a) and 3(b) show SEM images of porous Si samples after PtSi formation before and after the excess unreacted Pt has been removed, respectively, and Fig. 3(c) shows a cross-sectional SEM image of the sample after the excess unreacted Pt has been removed. A thin layer of gold was sputtered on the back of the n-Si samples for backside contacts. Our tests proved that this back side contact is ohmic. Figure 3(d) shows a simplified schematic of the pores with PtSi layer covering the walls and  $H_2S$  gas inside the pores.

The reverse bias currents of the fabricated porous Schottky diodes were compared with those of regular samples under similar experimental conditions. As with the results obtained elsewhere,<sup>(6)</sup> the reverse bias currents of our porous samples were observed to

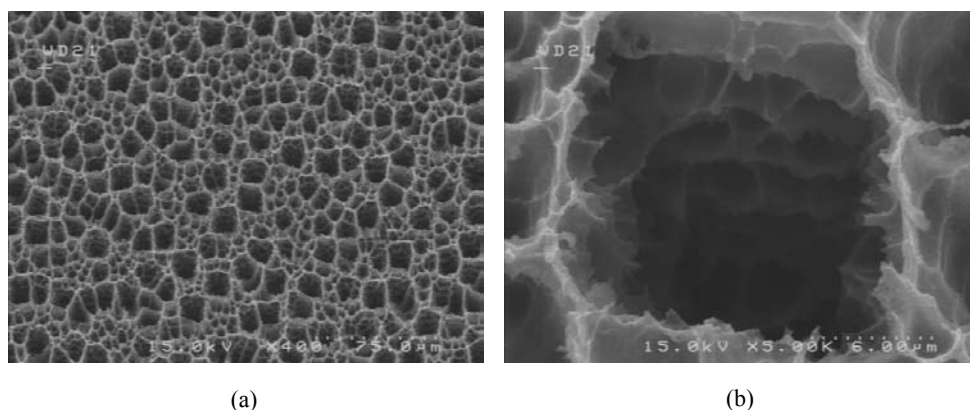


Fig. 2. (a) An SEM image of a porous Si sample and (b) an SEM image of a single pore.

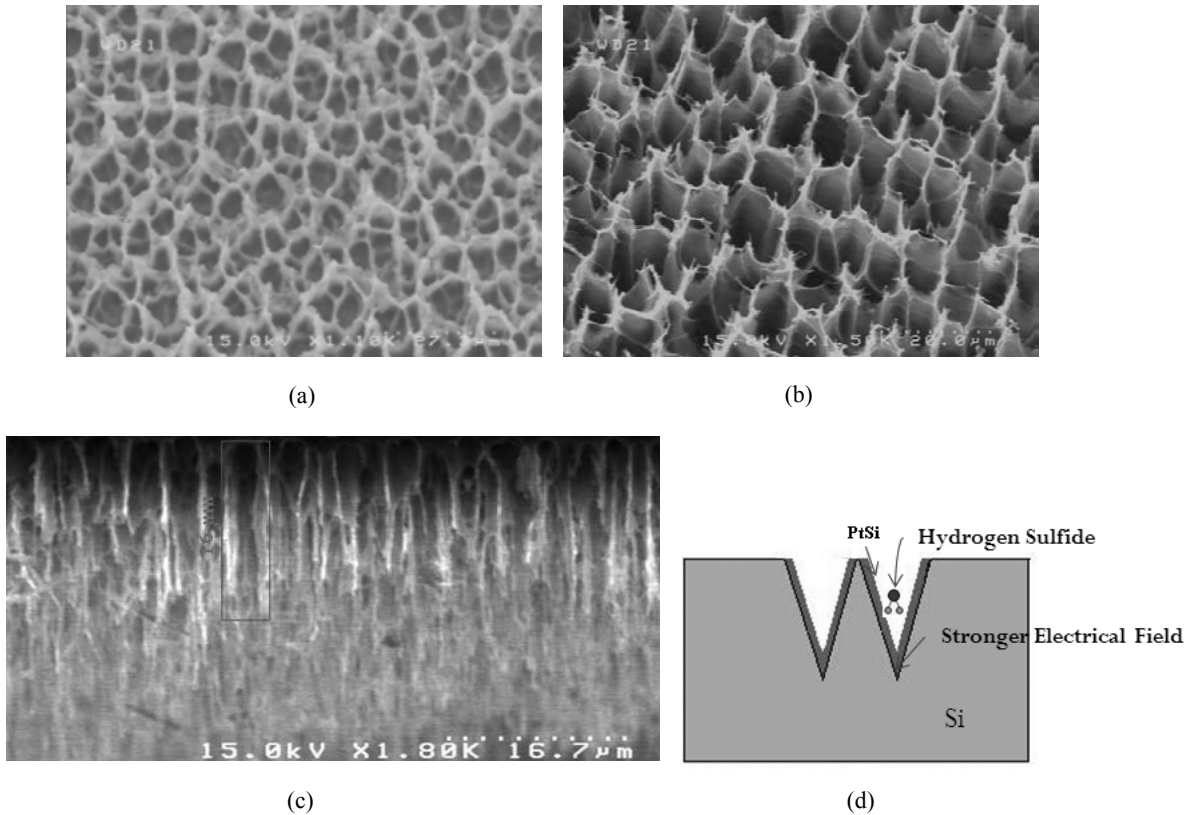


Fig. 3. SEM images of a porous Si sample after PtSi formation: (a) before the excess unreacted Pt is removed, (b) after the excess unreacted Pt is removed, (c) cross-sectional SEM image of a sample after the excess unreacted Pt is removed, and (d) a simplified schematic of the pores with PtSi layer covering the walls and H<sub>2</sub>S gas inside the pores.

be smaller than those of regular samples up to certain voltages and then increased beyond those of regular nonporous samples above those voltages.

H<sub>2</sub>S gas with different concentrations in N<sub>2</sub> was tested at room temperature. Figure 4(a) illustrates the room-temperature *I-V* characteristics of the sensor for various H<sub>2</sub>S concentrations at the flow rate of 100 sccm. The breakdown voltage of the sensor is reduced as the H<sub>2</sub>S concentration is increased, but it does not show a clear distinction among the H<sub>2</sub>S concentrations of smaller than 10 ppm at room temperature.

The same result was obtained for the higher flow rate of 1000 sccm at room temperature. The sensor sensed the H<sub>2</sub>S gas, but as shown in Fig. 4(b), the distinction between small concentrations such as 1 and 10 ppm was poor.

The responses of the sensor to another polar gas (CO) and a nonpolar gas (CH<sub>4</sub>) were also examined for comparison purposes as shown in Fig. 4(c). The concentration of these gases was fixed at 50 ppm. Only one gas plus nitrogen were allowed to enter the

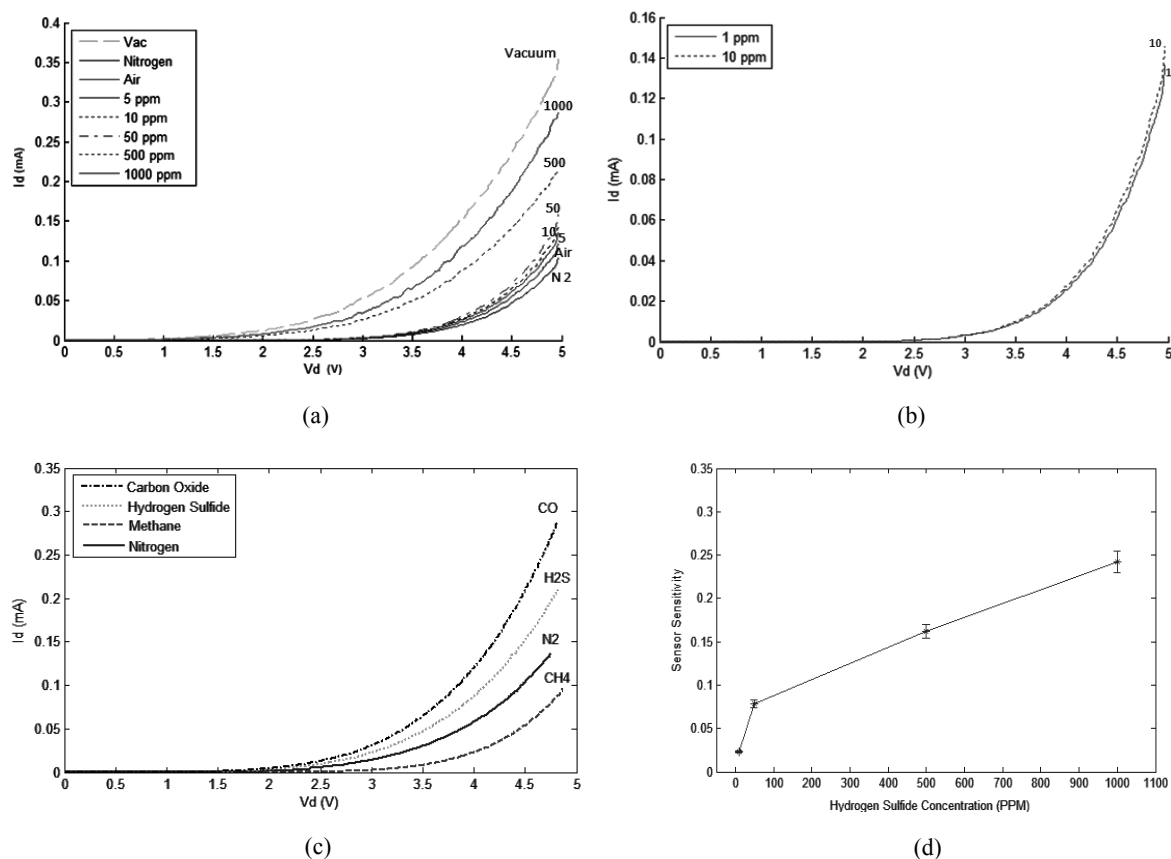


Fig. 4. (a)  $I$ - $V$  characteristics of the sensor for vacuum,  $N_2$ , air, and several  $H_2S$  concentrations in air at room temperature with flow rate = 100 sccm. (b)  $I$ - $V$  characteristics of the sensor for 1 and 10 ppm of  $H_2S$  concentrations in air at room temperature for flow rate = 1000 sccm. (c) Sensor's responses to 50 ppm of some polar ( $CO$  and  $H_2S$ ) and nonpolar gases ( $CH_4$  and  $N_2$ ) at room temperature with flow rate = 100 sccm. (d) Sensor's sensitivity for several  $H_2S$  concentrations in air at room temperature with flow rate = 100 sccm.

furnace each time and their  $I$ - $V$  characteristics were determined. The sensor's response to  $N_2$  is shown as the reference point. This sensor responds differently to different gases at room temperature.

At a fixed current level, the sensor's sensitivity as a function of  $H_2S$  concentration is defined as follows:

$$\text{Sensitivity} = (V_{\text{air}} - V_{\text{ppm}})/V_{\text{air}} \quad (2)$$

Figure 4(d) shows the sensitivity of the sensor to various  $H_2S$  concentrations at room

temperature. Voltages are measured at an arbitrary current of 0.1 mA. This test is repeated for other temperatures (50 and 80°C). Figure 5(a) illustrates the  $I$ - $V$  characteristics of the sensors with respect to various concentrations of  $H_2S$  gas at 50°C. Figure 5(b) illustrates the sensor's response to small concentrations of the  $H_2S$  gas at 50°C. As shown, the sensor is able to detect 1 ppm of the  $H_2S$  gas at 50°C. Figures 5(c) and 5(d) show the sensor's responses and sensitivity at 50°C, respectively. The responses of the sensor to another polar gas (CO) and a nonpolar gas ( $CH_4$ ) at 50°C are shown in Fig. 5(c) for comparison purposes. The concentration of these gases was fixed at 50 ppm. Only one gas plus nitrogen were allowed to enter the furnace each time and their  $I$ - $V$  characteristics were determined. The sensor's response to  $N_2$  is shown as the reference point. This

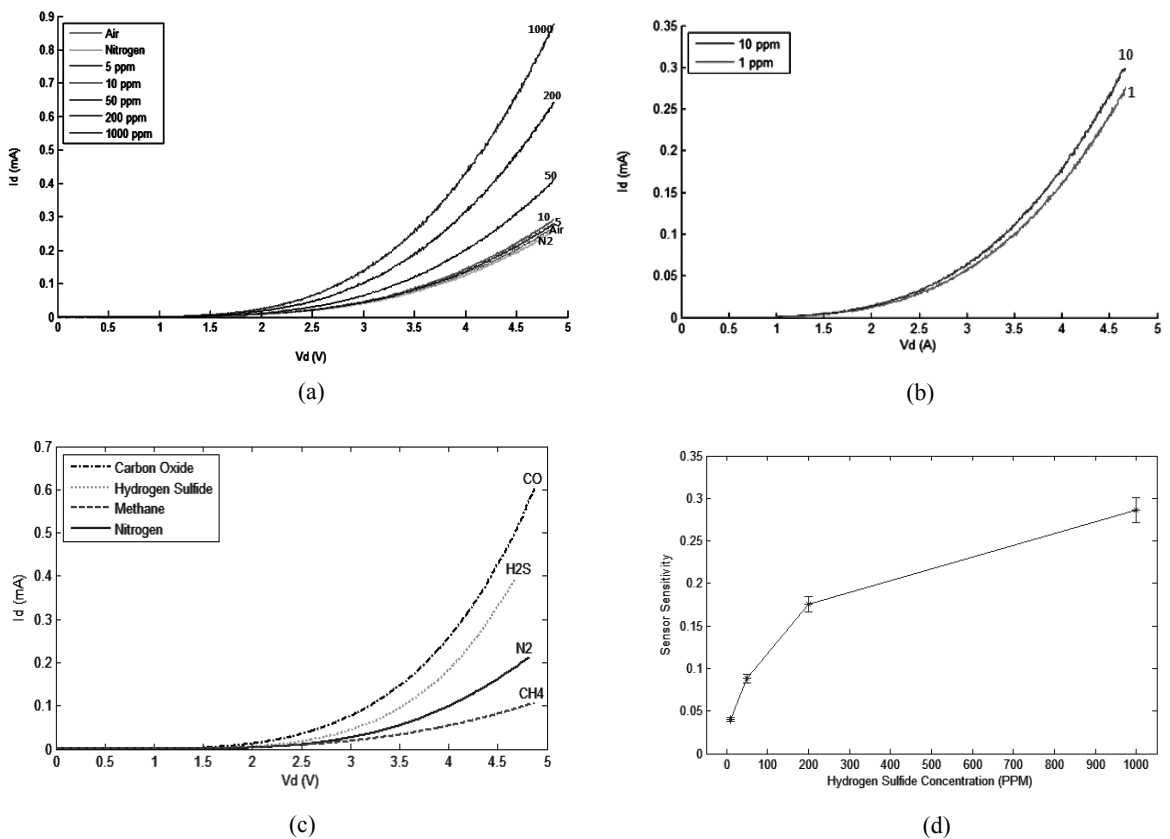


Fig. 5. (a)  $I$ - $V$  characteristics of the sensor for various  $H_2S$  concentrations in air at 50°C with flow rate = 100 sccm. (b)  $I$ - $V$  characteristics of the sensor for small  $H_2S$  concentrations in air at 50°C with flow rate = 1000 sccm. Small concentrations such as 1 and 10 ppm are clearly distinguishable from each other at this temperature. (c) Sensor's responses to 50 ppm of some polar (CO and  $H_2S$ ), and nonpolar gases ( $CH_4$  and  $N_2$ ) at 50°C with flow rate = 100 sccm. (d) Sensor's sensitivity for several  $H_2S$  concentrations in air at 50°C with flow rate = 100 sccm.

sensor responds differently to different gases at this temperature.

A comparison between Figs. 5(d) and 4(d) shows that the sensor's sensitivity is improved at 50°C.

Figure 6(a) shows the  $I$ - $V$  characteristics of the sensor with respect to various concentrations of  $H_2S$  gas at 80°C. As shown in Fig. 6(b), the sensor responds to 1 ppm of the  $H_2S$  gas at 80°C. Figures 6(c) and 6(d) show the sensor's responses and sensitivity at 80°C, respectively. The responses of the sensor to another polar gas (CO) and a nonpolar gas ( $CH_4$ ) at 80°C are shown in Fig. 6(c) for comparison purposes. The concentration of these gases was fixed at 50 ppm. Only one gas plus nitrogen were allowed to enter the furnace each time and their  $I$ - $V$  characteristics were determined. The

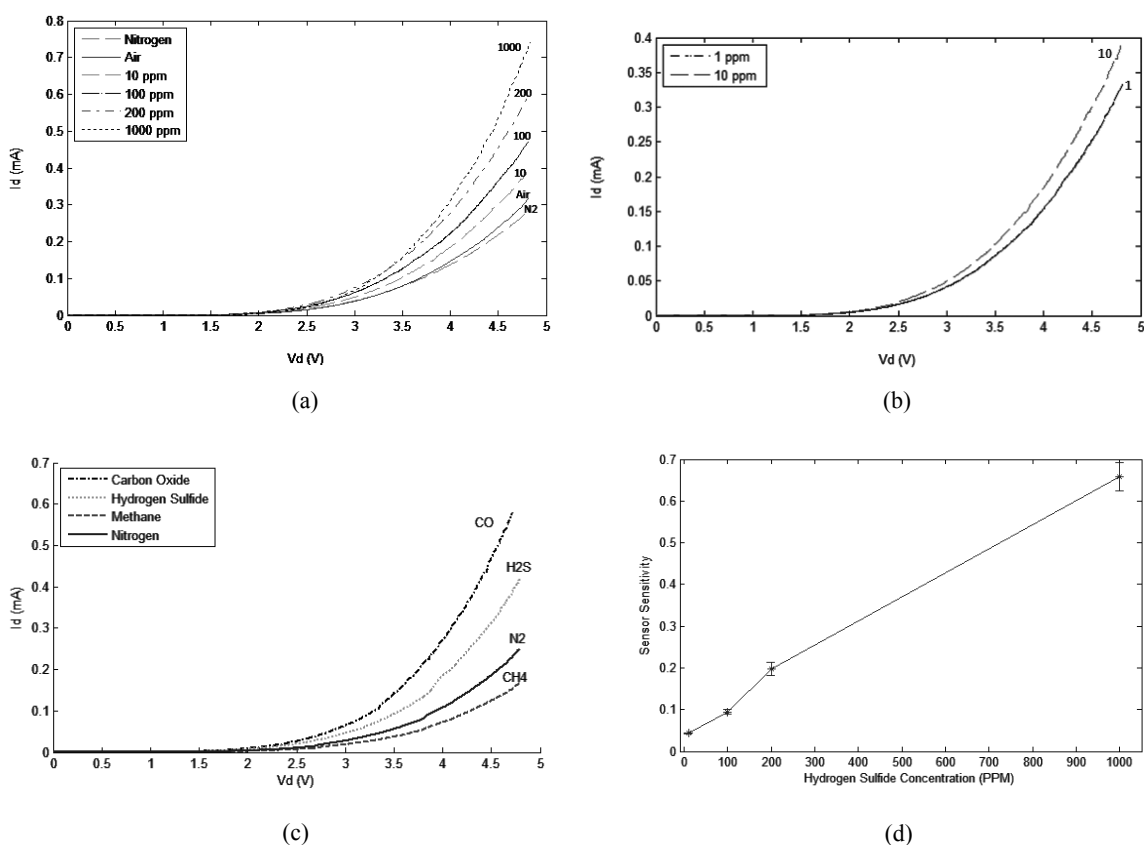


Fig. 6. (a)  $I$ - $V$  characteristics of the sensor for various  $H_2S$  concentrations in air at 80°C with flow rate = 100 sccm. (b)  $I$ - $V$  characteristics of the sensor for small  $H_2S$  concentrations in air at 80°C with flow rate = 1000 sccm. Small concentrations such as 1 and 10 ppm are clearly distinguishable from each other. (c) Sensor's responses to 50 ppm of some polar (CO and  $H_2S$ ), and some nonpolar gases ( $CH_4$  and  $N_2$ ) at 80°C with flow rate = 100 sccm. (d) Sensor sensitivity for several  $H_2S$  concentrations in air at 80°C with flow rate = 100 sccm.



sensor's response to  $N_2$  is shown as the reference point. This sensor responds differently to different gases at this temperature. A comparison among Figs. 6(d), 5(d), and 4(d) shows that the sensor's sensitivity is improved further at  $80^\circ\text{C}$ . Figure 7 shows the repeatability of the sensor's performances at room temperature,  $50^\circ\text{C}$ , and  $80^\circ\text{C}$ . They show the  $\Delta v$  or the change in the breakdown voltage between vacuum and 10 ppm of the  $H_2S$  gas vs time, at an arbitrary current of 0.2 mA. The flow rate is kept at 100 sccm. They show that the sensor's performances are repeatable at these temperatures.

Figure 8 shows that for the temperatures used in this investigation, the change in the sensor's breakdown voltage as a measure of its sensitivity increases with temperature. The  $H_2S$  concentration of 10 ppm was arbitrarily used in this figure.

The response times of the sensors fabricated in this investigation were calculated by obtaining the  $I$ - $V$  characteristic of the sensor at one concentration of  $H_2S$  and changing the concentration of the  $H_2S$  gas to another value and measuring the time that the sensor took to display a stable  $I$ - $V$  curve for the latter concentration of  $H_2S$ . The response times are shown in Fig. 9 (the rising portion of the curves). The response time decreased with the  $H_2S$  concentration and was in the range of 3 to 10 s for the  $H_2S$  concentrations used in this work. The recovery time of the sensor vs  $H_2S$  concentration is also shown in Fig. 9 (the falling portion of the curves). The recovery time increased with the  $H_2S$  concentration and was in the range of 20 to 45 s for the  $H_2S$  concentrations used in this investigation.

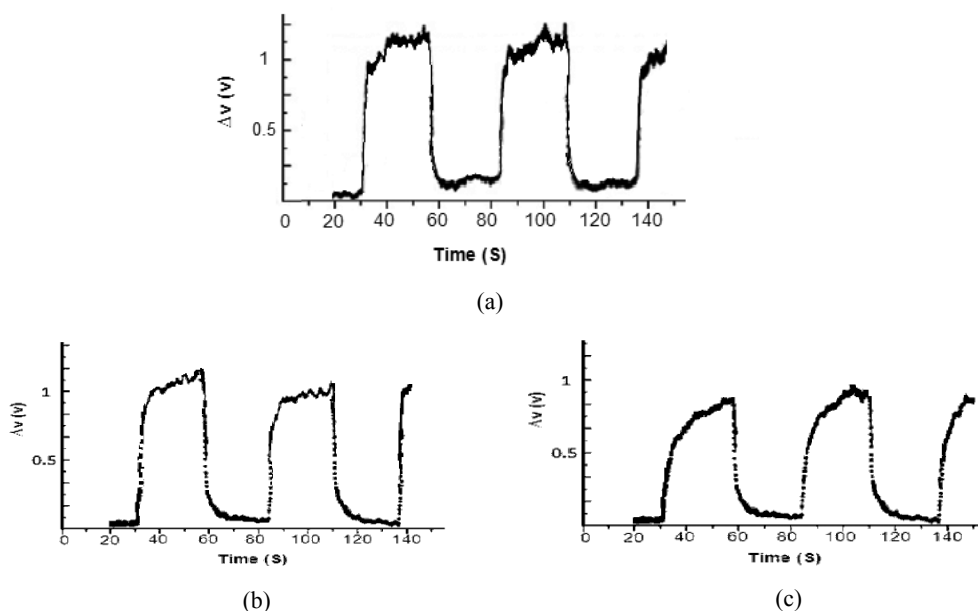


Fig. 7. Repeatability of the sensor's performances at (a) room temperature, (b)  $50^\circ\text{C}$ , and (c)  $80^\circ\text{C}$ .  $\Delta v = V_{\text{ppm}} - V_{\text{vac}}$  is the change in the breakdown voltage between vacuum and 10 ppm of the  $H_2S$  gas at an arbitrary current of 0.2 mA. The sensor's performance is repeatable at these temperatures. Flow rate = 100 sccm.

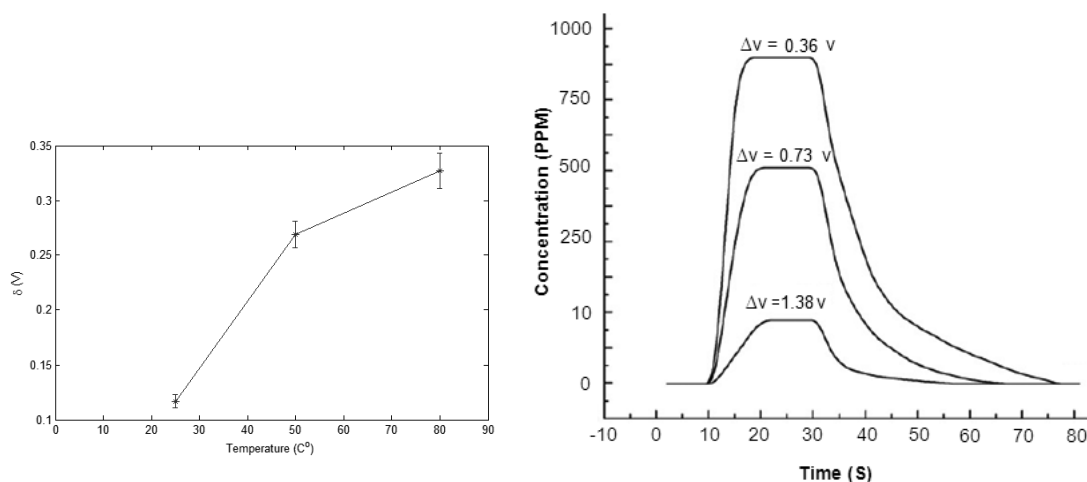


Fig. 8 (left). Change in the sensor's breakdown voltage as a measure of its sensitivity to 10 ppm of  $\text{H}_2\text{S}$  gas at room temperature,  $50^\circ\text{C}$ , and  $80^\circ\text{C}$ .

Fig. 9 (right). Response times and recovery times of the sensor for different  $\text{H}_2\text{S}$  concentrations in air at room temperature under the atmospheric pressure with flow rate = 100 sccm.  $\Delta v = V_{\text{ppm}} - V_{\text{vac}}$  at 0.2 mA.

#### 4. Discussion

As with the results obtained elsewhere,<sup>(6)</sup> despite the fact that the effective junction area of the porous Schottky structure is much more than that of a regular (nonporous) structure, the reverse bias currents of our porous samples were observed to be smaller than those of regular (PtSi/nonporous n-Si) structures up to certain voltages and then increased sharply and beyond those of the regular nonporous samples above those voltages. This is a strong indication that the single-electron or the Coulomb blockade effect is taking place in the PtSi/porous Si Schottky diode sensor structure. The depletion (junction) capacitances of the Schottky PtSi/porous n-Si junctions have been calculated to be on the order of  $10^{-19}$  to  $10^{-20}$  F even though their junction area is very large.<sup>(5)</sup> A threshold voltage of  $V_{\text{th}} = q/C$  is needed to send an electron from the Fermi level of the PtSi contact to the junction capacitor. This threshold voltage could be as large as 1.6 V for a PtSi/porous Si structure with the junction capacitance of  $C = 1 \times 10^{-19}$  F. Below this threshold voltage, no electron can enter the capacitor from the metal (PtSi) contact. That is why the reverse bias current of the PtSi/porous n-Si structure was observed to be smaller than that of the regular (PtSi/nonporous n-Si) structures up to the diode's threshold voltage and then increased sharply and beyond that of the regular nonporous sample when the reverse bias voltage exceeded the threshold voltage. The increase in the reverse bias breakdown current (or the decrease in the reverse bias breakdown voltage) of the porous structures can be explained by the impact ionization or avalanche

multiplication mechanism that seems to take place in the junction capacitance of the PtSi/porous Si metal-semiconductor structure after an electron is allowed to enter the capacitor. The breakdown voltage of the PtSi/porous n-Si junctions is related to the strength of the fringing electric fields at the tips and edges of the pores. The electric fields that porous samples create have been calculated using numerical methods, and the increase in the electric field by several orders of magnitude as compared with that of regular smooth PtSi junctions has been verified.<sup>(5)</sup> Such large electric fields enhance the avalanche breakdown mechanism. When the single-electron and subsequently the avalanche multiplication mechanisms take place, the reverse bias current of the diode increases even at room temperature. When a polar gas such as CO or H<sub>2</sub>S, which has internal dipole moments, fills the pores, its dipoles line up in the direction of the electric field and affect the fringing field distribution and magnitude and lower the breakdown voltage of the sensors with respect to vacuum or nonpolar gases, which lack polar components. Larger concentrations of polar gases replace more N<sub>2</sub> gas or air inside the pores and yield lower breakdown voltages.<sup>(7)</sup> Below the threshold voltages, the reverse bias currents of the porous samples were smaller than those of regular samples despite the fact that large electric fields decrease the depletion region of the junction to such a small width that tunneling of electrons can occur. Therefore, the Coulomb blockade or single-electron effect plus the impact ionization mechanism are considered to be the most reasonable explanation for this behavior. Such mechanisms can explain the room-temperature gas sensing ability of these diodes.

Depending on the sensor type, sensing mechanism, gas type, and its concentration, each sensor has an optimum operating temperature. For the temperatures tested in this investigation, the sensor's response or its ability to detect 1 ppm of the H<sub>2</sub>S gas (to distinguish it from 10 ppm of the gas) was improved with temperature and was best at 80°C. This could be because, at this temperature, the adsorption rate of gas molecules was higher than the adsorption rates at room temperature, and at 50°C.

To observe a stable voltage shift in the presence of a gas, a significant portion of the pores must be filled with the gas. A large concentration of H<sub>2</sub>S in N<sub>2</sub> or in air provides an adequate number of gas molecules inside the pores in a shorter period of time than a smaller concentration of the gas. This could be the reason for the observed decrease in the response time of the sensor as the H<sub>2</sub>S concentration was increased. Furthermore, it takes a longer time to remove a larger concentration of the H<sub>2</sub>S gas molecules from the pores than a small concentration of the gas. Therefore, the recovery time increases with the gas concentration.

Although this sensor responds differently to different polar and nonpolar gases, the main objective of designing this sensor was to sense the H<sub>2</sub>S gas with different concentrations in an environment such as the petroleum industry where this gas is predominantly present and is used to produce products such as sulfur and sulfuric acid. If there is more than one type of gas in an environment at the same time, the sensor does not determine how much concentration of what gas is present. That is the subject of a future work.

## 5. Conclusions

PtSi/porous n-Si Schottky diode gas sensors were fabricated for H<sub>2</sub>S gas sensing at the room temperature and at the elevated temperatures of 50 and 80°C. A quartz furnace was designed and built to test the sensors. The breakdown voltage of the sensor was reduced as the H<sub>2</sub>S concentration in N<sub>2</sub> was increased. The sensor was able to respond to 1 ppm concentration of H<sub>2</sub>S in N<sub>2</sub> at 50 and 80°C and to larger concentrations such as 10 ppm at room temperature.

The sensor's sensitivity was improved with the H<sub>2</sub>S concentration and with the temperature.

The sensor's response time was improved (decreased) and its recovery time was increased with the H<sub>2</sub>S concentration. The response times were in the range of 3 to 10 s, and the recovery times were in the range of 20 to 45 s. Furthermore, for the temperatures used in this investigation, the response of the sensor was improved with temperature.

Although the sensor responded differently to different polar and nonpolar gases, sensing H<sub>2</sub>S gas in an environment where this gas is predominantly present was the main objective of designing this sensor. Identifying different gases that are present at the same time was beyond the scope of this study.

The Coulomb blockade or single-electron effect is believed to be the most reasonable explanation for the room-temperature gas sensing ability of these diode sensors.

Finally, the low-temperature sensing capability and relatively fast response of the sensor to the examined gases are indications that the gas sensing mechanism of this Schottky diode PtSi/porous Si sensor is most likely a physical mechanism.

## Acknowledgements

This research was supported and funded by the Research Institute Petroleum Industrial (RIPI).

## References

- 1 AIHA: Emergency Response Planning Guideline for Hydrogen Sulfide, American Industrial Hygiene Association Set 6 (Akron, 1991).
- 2 CARB: Air Toxics Emissions Data Collected in the Air, Toxics Hot Spots Program, CEIDARS Database (January 29, 1999).
- 3 R. S. Niranjani, K. R. Patil, S. R. Sainkar and I. S. Mulla: *Mater. Chem. Phys.* **80** (2003) 250.
- 4 T. Hoyodo: *ECS Trans.* **16** (2008) 317.
- 5 F. Raissi, M. S. Abrishamian and T. Emadi: *IEEE Trans. Electron Devices* **51** (2004) 339.
- 6 F. Raissi and M. M. Far: *IEEE Sens. J.* **2** (2002) 476.
- 7 F. Raissi, S. Mirzakuchaki, H. M. Jalili and A. Erfanian: *IEEE Sens. J.* **6** (2006) 146.
- 8 R. L. Smith and S. D. Collins: *J. Appl. Phys.* **71** (1992) R1.
- 9 S. Khatami, H. Akrami and A. Fattah: *Defect and Diffusion Forum* **316** (2011) 81.
- 10 H. Wei, H. Sun, S. Wang, G. Chen, Y. Hou, H. Guo and X. Ma: *J. Nat. Gas Chem.* **19** (2010) 393.